

Phase-dependent outbreak dynamics of geometrid moth linked to host plant phenology

Jane U. Jepsen, Snorre B. Hagen, Stein-Rune Karlsen and Rolf A. Ims

Proc. R. Soc. B 2009 **276**, 4119-4128 first published online 9 September 2009
doi: 10.1098/rspb.2009.1148

References

This article cites 53 articles, 4 of which can be accessed free

<http://rsjb.royalsocietypublishing.org/content/276/1676/4119.full.html#ref-list-1>

Subject collections

Articles on similar topics can be found in the following collections

[ecology](#) (1123 articles)

Email alerting service

Receive free email alerts when new articles cite this article - sign up in the box at the top right-hand corner of the article or click [here](#)

To subscribe to *Proc. R. Soc. B* go to: <http://rsjb.royalsocietypublishing.org/subscriptions>

Phase-dependent outbreak dynamics of geometrid moth linked to host plant phenology

Jane U. Jepsen^{1,2,*}, Snorre B. Hagen¹, Stein-Rune Karlsen³
and Rolf A. Ims¹

¹Department of Biology, University of Tromsø, N-9037 Tromsø, Norway

²Polar Environmental Centre, Norwegian Institute for Nature Research, N-9296 Tromsø, Norway

³Norut, Northern Research Institute Tromsø, PO Box 6424, N-9294 Tromsø, Norway

Climatically driven Moran effects have often been invoked as the most likely cause of regionally synchronized outbreaks of insect herbivores without identifying the exact mechanism. However, the degree of match between host plant and larval phenology is crucial for the growth and survival of many spring-feeding pest insects, suggesting that a phenological match/mismatch-driven Moran effect may act as a synchronizing agent.

We analyse the phase-dependent spatial dynamics of defoliation caused by cyclically outbreaking geometrid moths in northern boreal birch forest in Fennoscandia through the most recent massive outbreak (2000–2008). We use satellite-derived time series of the prevalence of moth defoliation and the onset of the growing season for the entire region to investigate the link between the patterns of defoliation and outbreak spread. In addition, we examine whether a phase-dependent coherence in the pattern of spatial synchrony exists between defoliation and onset of the growing season, in order to evaluate if the degree of matching phenology between the moth and their host plant could be the mechanism behind a Moran effect.

The strength of regional spatial synchrony in defoliation and the pattern of defoliation spread were both highly phase-dependent. The incipient phase of the outbreak was characterized by high regional synchrony in defoliation and long spread distances, compared with the epidemic and crash phase. Defoliation spread was best described using a two-scale stratified spread model, suggesting that defoliation spread is governed by two processes operating at different spatial scale. The pattern of phase-dependent spatial synchrony was coherent in both defoliation and onset of the growing season. This suggests that the timing of spring phenology plays a role in the large-scale synchronization of birch forest moth outbreaks.

Keywords: population synchrony; forest insects; spread distance distributions; spring phenology; defoliation; MODIS-NDVI

1. INTRODUCTION

Herbivore populations with cyclic population dynamics sometimes exhibit high-density outbreaks that have devastating impacts on their food plants. Understanding the circumstances that permit such outbreaks has been a long-standing issue in ecology. In particular, some species of forest insects have become renowned for exhibiting population outbreaks (Myers 1988; Berryman 1996). Forest insect outbreaks are often regional in the sense that large tracts of forest are defoliated simultaneously, although the spatial outbreak extent may show substantial variation in both time and space for a given species (Liebhold & Kamata 2000). Analyses of spatio-temporally patterned outbreak dynamics may yield important insights into the underlying population dynamical processes (Liebhold *et al.* 2004).

Generally there are two approaches that may be adopted for analysing spatio-temporal data on herbivore outbreaks. One approach focuses on the concept of

population synchrony, defined as the correlation in population rate of change between sites within a population's distribution range (Bjørnstad *et al.* 1999; Liebhold *et al.* 2004). Central to this approach is to assess how synchrony depends on distance. Of interest is also whether such synchrony–distance relations (often estimated in terms of spatial autocorrelograms) is anisotropic (i.e. directionally dependent) in the sense that they change in space or time (Bjørnstad *et al.* 1999). Spatial changes may imply environmental gradients (Hagen *et al.* 2008) or nonlinear endogenous dynamics giving rise to complex spatio-temporal patterns (Sherratt & Smith 2008). Temporal changes may take the form of *phase-dependent synchrony* (Haydon *et al.* 2003), meaning that the degree of synchrony differs between the increase, peak and crash phase of the outbreak cycle. Such phase-dependency can be indicative of which processes promotes outbreaks.

The other approach focuses on the analysis of the *rate of spread* of outbreaks. This is the natural approach in the studies of outbreaking invasive species (e.g. Tobin *et al.* 2007). In that case the rate of spread, as quantified by the distribution of spread distances, is likely to be directly related to the dispersal distance distribution of the

* Author and address for correspondence: Polar Environmental Centre, Norwegian Institute for Nature Research, N-9296 Tromsø, Norway (jane.jepsen@nina.no).

invasive species. Although the 'rate of spread approach' also may be applied to species exhibiting spatially extensive outbreak dynamics within their native range, the underlying processes are more elusive since various population and community processes (other than dispersal) may be involved. Nevertheless, modelling the distribution of spread distances may give clues to what are the most likely underlying processes, in particular, when conducted in combination with the more conventional analysis of population synchrony.

In this study we apply both approaches to a severe outbreak of birch forest geometrids in northern Fennoscandia. The two geometrid moth species in question, *Epirrita autumnata* and *Operophtera brumata*, exhibit cyclic outbreak dynamics, which sometimes leads to spatially extensive defoliation of the mountain birch forest in this region (Tenow 1972; Ruohomäki *et al.* 2000; Tanhuanpää *et al.* 2002). The outbreak cycles have often been assumed to be on a sufficiently large scale to be explained by a regionalized Moran effect (Berryman 1996; Ruohomäki *et al.* 2000). Among several possible mechanisms that may underlie Moran effects, variable spring temperatures causing a varying degree of matching in the phenologies of moth and their host plant (i.e. birch) have recently been highlighted for the insect–host plant system in question (Stenseth & Mysterud 2002; van Asch & Visser 2007; Hagen *et al.* 2008). As phenological patterns are observed to be structured according to latitudinal and altitudinal gradients (Karlsen *et al.* 2008), as well as topographical features, such a phenological mismatch-driven Moran effect could also be responsible for the more complex spatial dynamics recently reported for birch forest moths (Klemola *et al.* 2006; Tenow *et al.* 2007). Yet, other studies have hinted that dispersal (either in the moths or their enemies) may be important, at least under some circumstances (Ims *et al.* 2004). Previous studies of spatio-temporal dynamics of birch forest geometrids have been analysed according to the population synchrony approach (Klemola *et al.* 2006; Tenow *et al.* 2007; Hagen *et al.* 2008).

Here we present, to our knowledge, the first analysis of spatio-temporal herbivore outbreak dynamics with a particular reference to food plant phenology as a putative Moran effect. Our analyses are facilitated by regional satellite-derived time series of forest defoliation caused by the moth as well as phenology of their host plant covering all phases of an outbreak cycle. Owing to their extensive spatial coverage, such time series provides better opportunities for comprehensive analyses than the spatially restricted and scattered ground-based population count data which so far has formed the basis for such analyses.

The goal of our study is threefold. First, we use both the analytical approaches outlined above to establish to what extent patterns of population synchrony and patterns of outbreak (i.e. defoliation) spread are linked. We use the term 'spread' in the widest possible sense, knowing well that the mechanism(s) operating behind the observed spatial dynamics does not necessarily include actual dispersal of individual moths. By spread we refer to any between-year change in the spatial distribution of outbreaks. Second, we evaluate whether these spatial processes are dependent on the phase of the outbreak cycle. Finally, we examine whether there is any spatial phase-dependent coherence between the moth outbreaks and birch phenology, expressed as the timing of onset of the

growing season; i.e. thus evaluating if the degree of matching between the phenology of the moth and their host plant could act as a Moran effect.

2. MATERIAL AND METHODS

(a) Study system

In the present study we consider Fennoscandia north of 68° N (figure 1). We delineate the study region to the east by the approximate birch/mixed birch-coniferous forest limit, a total area of about 106700 km² of which roughly 30 per cent is forested. Northern Fennoscandia lies in the arctic/alpine-boreal transition zone and includes the northern parts of Norway, Sweden and Finland. The Scandinavian mountain chain (the Scandes) divides the area into a humid oceanic region along the western coast, and a dry continental region to the southeast. Birch (*Betula pubescens*, Ehrh.) forests dominate the lowland, except in the southeast where dominance gradually shifts to conifers. In the western region, wind-protected areas are characterized by tall birch forest types where herbs and ferns dominate the ground cover. By contrast, the continental east is characterized by low-growing and open, multi-stemmed birch forest types where lichen and crowberry dominate the ground cover. Throughout the whole region, intermediate bilberry birch forest types cover large areas (Hämet-Ahti 1963; Väre 2001; Johansen & Karlsen 2005).

In the northern boreal birch forests of Fennoscandia, winter moth and autumnal moth are the most important cause of disturbance. Both species exhibit cyclic population outbreaks at approximately 10 year intervals in this region (Tenow 1972; Haukioja *et al.* 1988; Bylund 1999). The two species, when occurring in sympatry within their outbreak range, exhibit largely synchronous dynamics, with winter moth dominating at termination of the outbreaks (Tenow *et al.* 2007; Klemola *et al.* 2008). The cyclicity of the outbreaks is documented in qualitative historical records as far back as the 1860s (Tenow 1972; Nilssen *et al.* 2007). Individual outbreaks vary greatly in amplitude, duration and spatial extent (Tenow 1972; Ruohomäki *et al.* 2000; Klemola *et al.* 2006; Tenow *et al.* 2007). The outbreaks can be massive and have dramatic effects, with severe defoliation over vast areas and occasionally death of the forest (Tenow 1972; Kallio & Lehtonen 1973; Lehtonen & Heikkinen 1995; Tenow & Bylund 2000). Defoliation of birch by geometrids in this region is of a seasonal character. The larvae hatch in approximate synchrony with budburst (late May—early June in northern Fennoscandia). The feeding periods last for four to eight weeks depending on the temperature and forage quality (Ruohomäki *et al.* 2000) after which the larvae drop to the ground and pupate in the soil. At high larval densities a large proportion of birch leaves are consumed at the bud stage and never unfold. After severe defoliation there is little or no refoliation during the same growing season.

(b) Estimates of annual defoliation

Historically, no systematic monitoring of the extent and distribution of forest damage caused by geometrids in northern Fennoscandia has ever been in place. Recently however, Moderate Resolution Imaging Spectroradiometer (MODIS) satellite imagery (the MOD13Q1 product; Huete *et al.* 2002) has been successfully used to map the annual distribution of defoliation in northern Fennoscandia covering

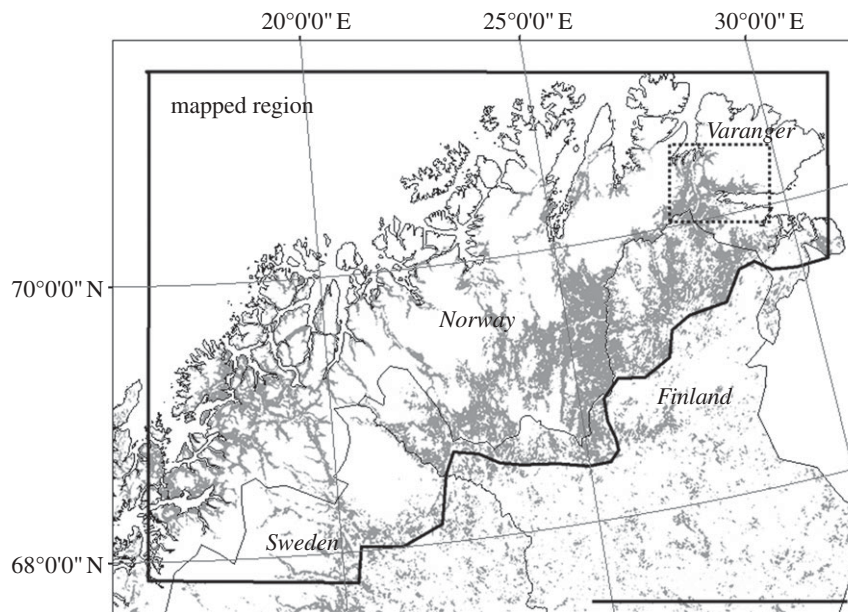


Figure 1. A map showing the extent of the mapped region in northern Fennoscandia. Grey shaded areas show the distribution of birch dominated forest in the region. The hatched square delineates the sub-region of Varanger for which a detailed depiction of the geometrid outbreak was made (see figure 6). Scale bar, 200 km.

the last 9 years (2000–2008) and a full outbreak cycle by geometrids in the region (Jepsen *et al.* 2009). Defoliation scores based on changes in summer normalized difference vegetation index (NDVI) were shown to be both a good proxy for local larval densities measured on the ground and an accurate predictor for the prevalence of defoliation when evaluated against independent data from other areas in the region (Jepsen *et al.* 2009).

The basic data for our analysis were time series of defoliation scores binned to produce annual maps of the presence/absence of severe defoliation using a threshold defoliation score. A threshold defoliation score of 14 per cent was shown to produce the most accurate discrimination between areas with and without visible defoliation (Jepsen *et al.* 2009). The spatial grain of the original data is 250×250 m determined by the grain of the satellite imagery used for the classification. In order to analyse patterns of spatial dynamics in defoliation we aggregated the 250 m presence/absence data into grid cells of increasing size from 6.25×6.25 km to 100×100 km containing the proportion of forested area in each grid cell predicted to be defoliated. We did this to assess whether our results were sensitive to the grain used in the analysis (*sensu* Wiens 1989).

(c) Estimates of annual onset of the growing season

Several studies have been devoted to developing and evaluating satellite-based approaches for mapping the onset and duration of the growing season in northern Fennoscandia in recent years (Karlsen *et al.* 2006, 2008; Beck *et al.* 2007). In the most recent approach (Karlsen *et al.* 2008), annual maps of the mean date for onset and end of the growing season for the years 2000–2006 were developed for the entire northern Fennoscandia based on the same MODIS-NDVI data used for mapping moth defoliation (Jepsen *et al.* 2009). The satellite-based time series of the onset of the growing season were shown to have a moderate-high correlation with the onset of leafing of birch from phenological stations distributed across northern Fennoscandia (Karlsen *et al.* 2008). This time series have since been extended to include 2007

(Karlsen *et al.* 2009). The spatial extent and grain was identical to the annual defoliation maps yielding a unique opportunity for comparative analysis of the spatial dynamics of defoliation and spring phenology across an entire region. In order to do so at varying spatial scales, we aggregated the original 250 m time series for the onset of the growing season into grid cells of increasing size from 6.25×6.25 km to 100×100 km containing the mean date for onset of the growing season in each grid cell.

(d) Analysis of spatial synchrony and defoliation spread

The presence and geographical scale of spatial synchrony between time series of defoliation as well as between time series of onset of the growing season were examined separately for each spatial grain (6.25–100 km) in R using non-parametric covariance functions (function ‘Snfc’ in library ‘nfc’, Bjørnstad *et al.* 1999; Bjørnstad & Falck 2001). We calculated spatial covariance functions of the entire time period (2000–2008 for defoliation, 2000–2007 for the onset of growing season) and for each of three phases of the outbreak cycle.

To characterize the distribution of spread distances through the outbreak cycle we calculated the straight-line distance from each defoliated pixel in year t to the nearest defoliated area in year $t - 1$ using the original 250×250 m pixels. To avoid noise from scattered single pixels we only considered distances to neighbours with a minimum area of 5 pixels (corresponding to an area of approx. 0.3 km^2). We compared the frequency distribution of observed spread distances to the distribution of distances between a random sample of forested pixels and the nearest defoliated area in a given year. Spread events with distance zero (e.g. recurring outbreaks in a pixel for two or more consecutive years) were excluded from the analysis.

Nonlinear models were fitted to the observed spread data and the least-square estimates of the model parameters estimated in R (the ‘nls’ function in library ‘stats’; Bates & Watts 1988). We compared the performance of four standard spread

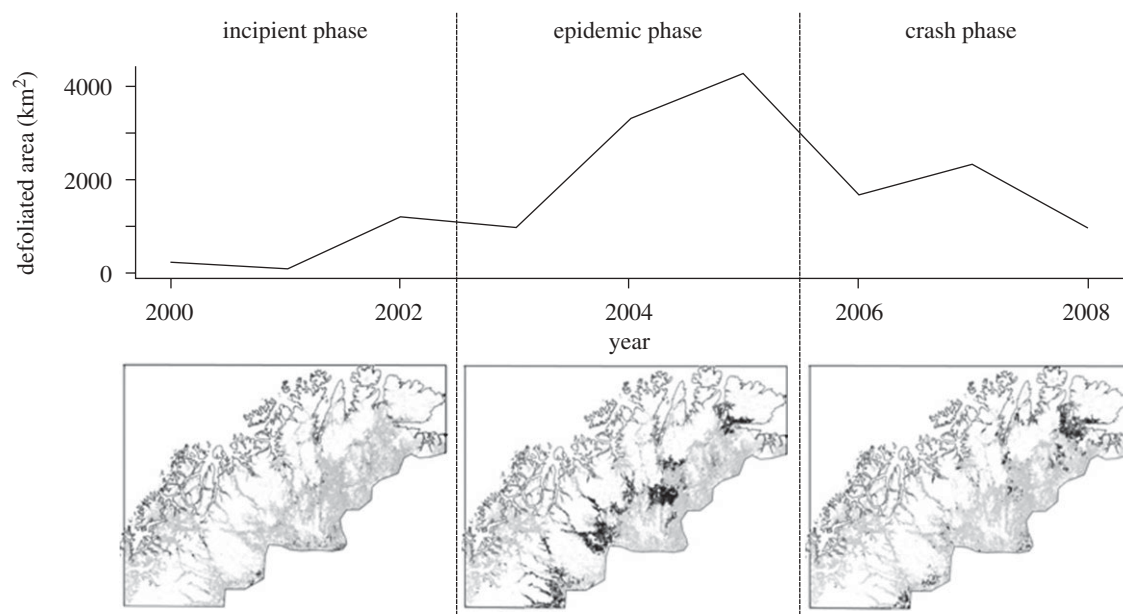


Figure 2. The total area of birch forest in the mapped region affected by severe defoliation annually for the years 2000–2008 (upper panel). The outbreak cycle was divided into three phases: the incipient, the epidemic and the crash phase. The lower panel shows the areas affected by severe defoliation during the three phases in black. The distribution of birch-dominated forest is shown in grey.

models: a simple diffusion model (termed ‘Diffusion’) in which the spread probability decrease with distance following a normal curve, a fat-tailed leptokurtic spread model (termed ‘Leptokurtic’), in which the probability for both very short and long distance spread is higher than in a diffusion model, and finally two fat-tailed stratified models which assumes a two-scale spread probability. The first is a diffusion–diffusion model (termed ‘StratifiedDD’), in which spread probability is described using two diffusion models operating at different scales, and the second a diffusion-leptokurtic model (termed ‘StratifiedDL’), which uses a short-range diffusion and a long-range leptokurtic model. The diffusion model describes the hypothetical situation where new defoliation spread out from existing defoliated areas at a constant spread rate. However, natural spread data are frequently characterized by fat-tailed distributions (Kot *et al.* 1996) owing to the presence of long-distance spread events, and leptokurtic and stratified dispersal kernels have repeatedly been shown to provide better estimates of the dispersal and spread of both native and invasive organisms (Kot *et al.* 1996; Chesson & Lee 2005; Johnson *et al.* 2006; Liebhold & Tobin 2008). Specifically, a stratified spread model is a likely candidate if the observed spread is determined by two independent mechanisms, for instance short-range dispersal (by flight or wind) coupled with long-range wind- or human-mediated dispersal (Liebhold *et al.* 1992; Sharov & Liebhold 1998; Gilbert *et al.* 2004), or a regionally synchronizing factor in the environment (a Moran effect).

3. RESULTS

(a) General characteristics of the outbreak

The total area estimated to be severely defoliated annually (figure 2, upper panel) show that a full outbreak cycle was completed during the years 2000–2008. The outbreak did not have a clearly defined epicentre, but rather began more or less simultaneously in multiple locations across the region (figure 2, incipient phase). Defoliation peaked in 2004–2005 during which 3–4000 km² of the birch forest

belt in the study region was affected by severe defoliation annually (10–15% of total birch forest area: figure 2, epidemic phase). The Varanger region in northeast Norway (outlined in figure 1) was most severely affected, with local defoliation lasting for 3–5 years in some places (as opposed to 1–3 years in most other regions). In the course of the outbreak cycle, a total area of just above 10 000 km² was affected by severe defoliation at least once, corresponding to one-third of the birch forest in the region.

Based on the regional evolution of the outbreak (figure 2) we defined the following three phases for the purpose of the analysis of synchrony and spread: (figure 2); *the incipient phase* (2000–2002) characterized by low, slowly increasing, prevalence of defoliation; *the epidemic phase* (2003–2005) during which the prevalence of defoliation increased dramatically and eventually peaked in the entire region and *the crash phase* (2006–2008 for defoliation, 2006–2007 for the onset of growing season) where the prevalence of defoliation diminished almost to pre-epidemic levels.

(b) Synchrony in outbreak and spring phenology

Spatial synchrony in the prevalence of defoliation was evident up to a distance of approximately 200 km (155–230 km depending on the grain; figure 3a). The regional synchrony (i.e. the average synchrony across the entire region) was generally low when considering the time series covering the whole outbreak period (figure 3a). A separate analysis of synchrony for each outbreak phase revealed a markedly higher regional synchrony in the incipient phase compared with later phases of the outbreak (figure 3b). This was owing to a steeper decay in synchrony with distance in the epidemic and crash phases than in the incipient phase. The pattern of spatial synchrony in the mean onset of growing season had some striking similarities to the patterns of moth defoliation. A strong local spatial synchrony was evident up to a distance of approximately 170 km (figure 3c).

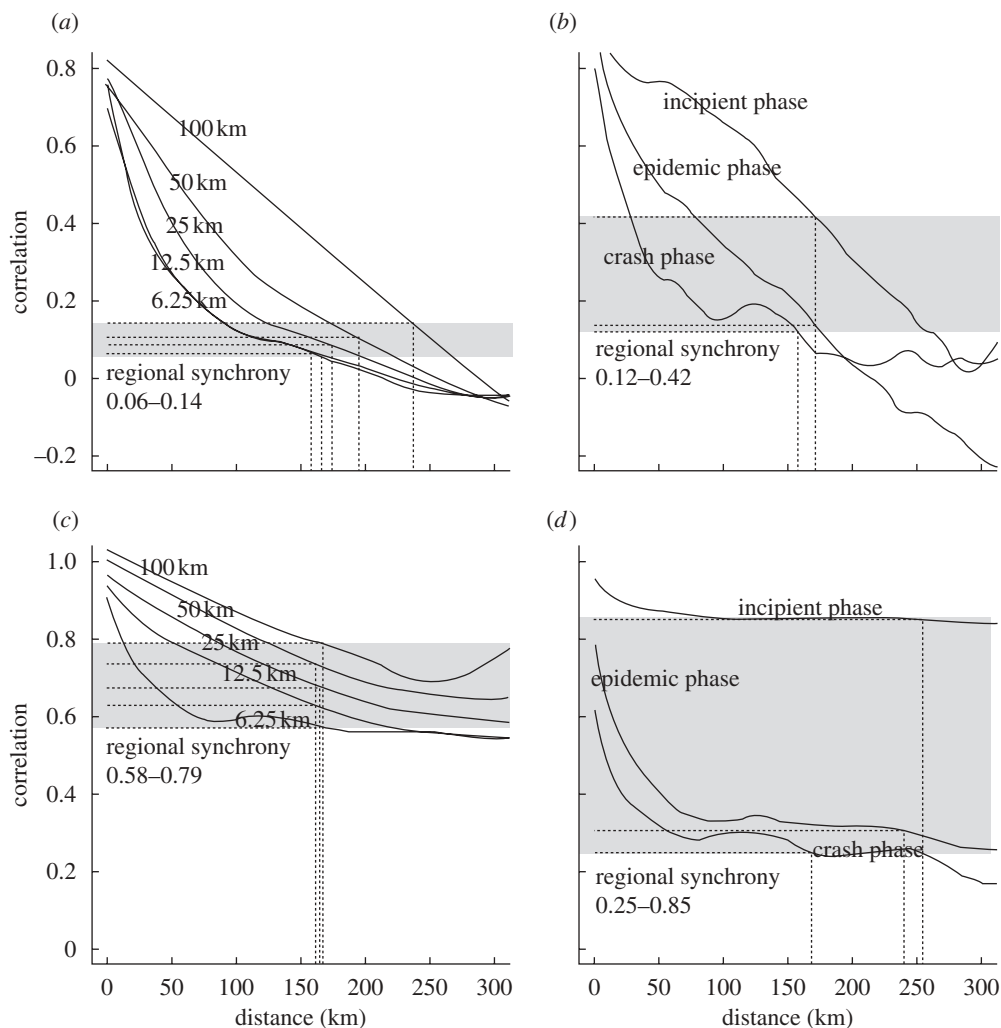


Figure 3. Non-parametric covariance functions (Bjørnstad & Falck 2001) showing synchrony-distance relations for both geometrid outbreaks and spring phenology. (a) Spatial synchrony of outbreaks over all outbreak phases for grid cells (grain) of increasing size (6.25×6.25 km– 100×100 km); (b) outbreak synchrony for the incipient, epidemic and crash phase of the outbreak calculated for the smallest grid cell size (6.25 km). The range of the regional average synchrony is shown as grey shaded bars. The geographical scale of synchrony (where the curve covariance function crosses the average regional synchrony) is shown by dashed lines; (c,d) corresponding figures for spatial synchrony in the mean onset of the growing season.

As for defoliation, the incipient phase of the outbreak (2000–2002) was characterized by a markedly higher regional synchrony in the onset of the growing season than the later phases of the outbreak (figure 3d). Generally however, a higher level of regional synchrony was present in the onset of the growing season than in defoliation, independent of spatial grain and outbreak phase.

(c) Spread of outbreaks

The distribution of distances between defoliated pixels and the closest defoliated area in the previous year was highly phase-dependent (figure 4). It decreased markedly as the outbreak progressed (spread distance in kilometres, median (interquartile range): incipient = 39.1 (39.1); epidemic = 4.5 (9.9); crash = 3.25 (13.3)). During the incipient phase (figure 4), intermediate spread distances (in the range 20–80 km) were over-represented when compared with a chance occurrence, while very long spread distances (100–150 km) were clearly under-represented. In the epidemic and crash phase, shorter spread distances (0–15 km) were strongly over-represented when compared with a chance occurrence.

The observed pattern of defoliation spread was best described as a two-scale stratified process, as the stratified spread models provided the best fit both to the data as a whole and to the epidemic/crash phase of the outbreak separately (table 1 and figure 5). The best fit was obtained using a stratified diffusion–leptokurtic model (StratifiedDL). This suggests that the spread of defoliation in this system is determined by two independent processes, a very short-range diffusion-like process and a fat-tailed long-range process.

Figure 6 shows a visual representation of the gradual spread of defoliation in the Varanger area in northeast Norway from 2002 to 2008 through the epidemic and crash phases of the outbreak. Defoliation in this region was particularly severe and long-lasting and hence provides a unique illustration of the short-range pattern of defoliation spread in the system. Spread distances ranged from 1–12 km between years and were larger during the early years of the outbreak (2002–2003). As the outbreak entered the crash phase, the advancing front of the spread became increasingly fuzzy and no good distinction can be made between 2007 and 2008.

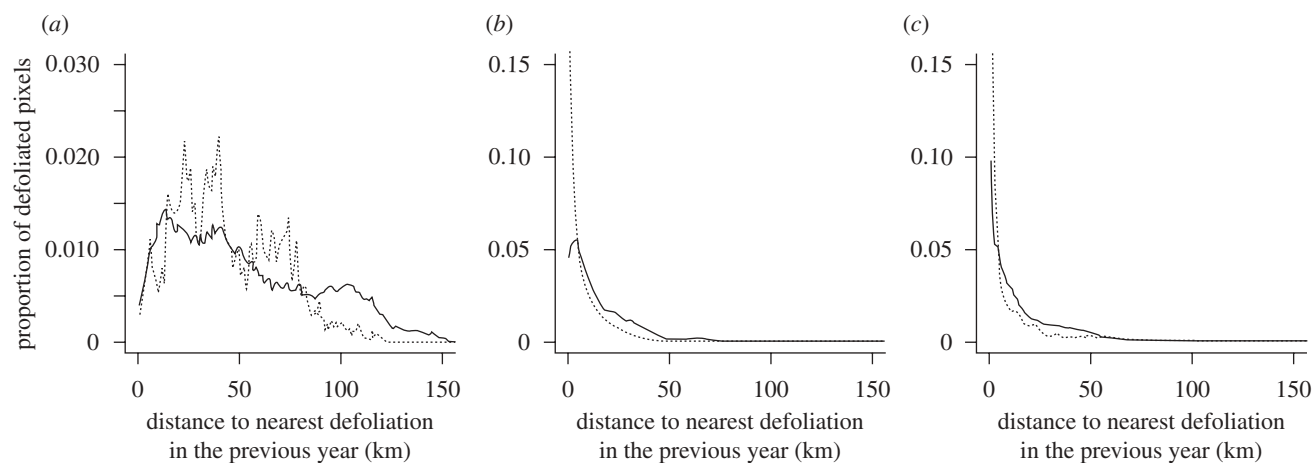


Figure 4. Frequency distribution of observed distances from defoliated pixels (dashed line) and a random sample of forested pixels (solid line, $n = 25\,000\text{ yr}^{-1}$) to the nearest defoliated area in the previous year during the (a) incipient ($n = 16\,509$, $n_{\text{random}} = 50\,000$), (b) epidemic ($n = 117\,690$, $n_{\text{random}} = 75\,000$) and (c) crash phase ($n = 54\,590$, $n_{\text{random}} = 75\,000$) of the outbreak.

Table 1. Parameters (see formulae in figure 5), 95 per cent confidence limits (CI) and fit statistics (Akaike Information criteria, AIC and log-likelihood, LL) for models fitted to the pooled data over all years (2000–2008) and separately to the incipient, epidemic and crash phase of the outbreak. (None of the standard spread models fitted well during the incipient phase of the outbreak. The stratified model based on a short-range diffusion and a long-range leptokurtic distribution (StratifiedDL) provided by far the best fit (lowest AIC/highest LL) to the observed defoliation spread distances during the epidemic and crash phase, as well as for the dataset as a whole.)

model	α	CI	β	CI	γ	CI	AIC	LL	d.f.
<i>all data</i>									
diffusion	0.09	[0.078;0.102]					-1241	623	2
leptokurtic	0.59	[0.58;0.61]					-1425	715	2
stratifiedDD	0.23	[0.20;0.25]	-1.5	[-1.58;-1.42]	0.004	[0.003;0.005]	-1844	926	4
stratifiedDL	0.73	[0.67;0.81]	0.25	[0.21;0.29]	0.73	[0.71;0.75]	-2397	1203	4
<i>incipient</i>									
diffusion	0.00024	[0.00021; 0.00027]					-211	107	2
leptokurtic	0.17	[0.16;0.19]					-190	97	2
stratifiedDD	n.a.	n.a.	n.a.	n.a.	n.a.	n.a.	n.a.	n.a.	n.a.
stratifiedDL	n.a.	n.a.	n.a.	n.a.	n.a.	n.a.	n.a.	n.a.	n.a.
<i>epidemic</i>									
diffusion	0.048	[0.043;0.054]					-1217	611	2
leptokurtic	0.54	[0.53;0.56]					-1354	679	2
stratifiedDD	0.16	[0.14;0.17]	-1.226	[-1.299;-1.155]	0.0046	[0.0041;0.0052]	-1864	936	4
stratifiedDL	1.80	[1.45;2.44]	0.58	[0.56;0.59]	0.767	[0.760;0.774]	-2527	1268	4
<i>crash</i>									
diffusion	0.22	[0.20;0.24]					-1505	755	2
leptokurtic	0.74	[0.71;0.77]					-1336	670	2
stratifiedDD	0.33	[0.31;0.35]	-2.09	[-2.18;-1.99]	0.0042	[0.003;0.005]	-1995	1002	4
stratifiedDL	0.50	[0.46;0.55]	-0.40	[-0.54;-0.26]	0.72	[0.67;0.78]	-2199	1104	4

4. DISCUSSION

(a) Phase-dependent and scale-specific outbreak spread and synchronization

Few studies on cyclic species have yet been dedicated to assess variation in spatial dynamics at different phases of the population cycle (Haydon *et al.* 2003; Aukema *et al.* 2006). Our investigation of defoliation patterns caused by cyclic geometrid moths in northern boreal birch forest provided evidence of highly phase-dependent spatial dynamics. The incipient phase of the outbreak was characterized by high regional synchrony, and long defoliation spread distances (up to approx. 80 km) between years. Later phases of the outbreak were characterized

by much lower regional synchrony and defoliation spread over much shorter distances (a few kilometres). Thus our results may suggest that the observed defoliation spread (and synchronization) was the result of two processes operating at different spatial scales and phases of cycle according to the following scenario: the outbreak was initiated in multiple locations simultaneously, possibly by a favourable environmental condition, which permits high local population growth rates over reasonably large areas. This gave rise to the long defoliation 'spread' distances, which cannot reasonably be attributed to moth dispersal *per se*. Thus the scale of population synchrony in this initial phase of the population cycle is

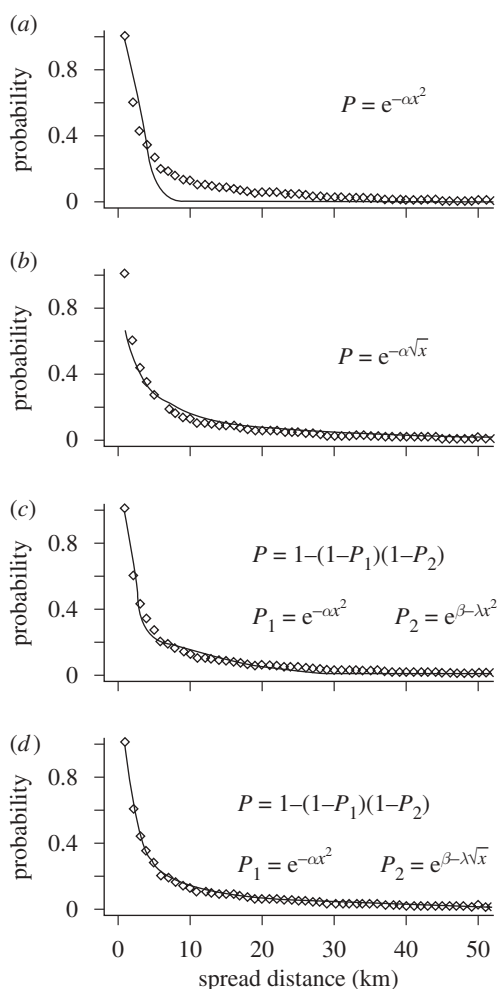


Figure 5. The four spread models (solid lines): (a) diffusion; (b) leptokurtic; (c) stratifiedDD; and (d) stratifiedDL, fitted to observed defoliation spread distances (diamonds) for pooled data over all years (2000–2008).

determined by the scale of the synchronizing factor in the environment. As the population cycle progresses, new outbreaks, and consequently, defoliation happens increasingly as a result of a gradual spread out from the existing defoliated areas. At this stage dispersal could have contributed more to the spread. This causes much shorter defoliation spread distances and lower regional synchrony during the epidemic and crash phase of the population cycle when compared with the incipient phase. However, even within the realm of the generally short-tailed spread distance distributions of the epidemic and crash phase, the best spread models suggested that two processes were operating, perhaps owing to a persistent effect of the processes that dominated in the incipient phase. Alternatively, the scale of synchrony could simply be set by the configuration of outbreaks during the incipient phase of the population cycle, which subsequently functions as ‘sources’ for new defoliation in the later phases of the cycle. In this manner a single favourable year could be influential to the spatial evolution of the entire outbreak.

Like most other studies addressing the spatial dimensions of cyclic outbreak dynamics, previous analyses of birch forest moths have focused solely on the issue of regional synchrony across the temporal extent of the study (Klemola *et al.* 2006; Tenow *et al.* 2007), thus

without attempting to partition out phase- or scale-dependent patterns and processes as we have done here. Nevertheless, the previous studies have concluded that although dispersal could not be ruled out as a contributing synchronizing mechanism (Ims *et al.* 2004), a regionalized climatic Moran effect is more likely. Our results comply with and extend on this conclusion. Mass-dispersal of larvae over long distances (as would be required to initiate new outbreaks) is probably limited, although the process is little studied under field conditions (Bell *et al.* 2005). Experimental studies of ballooning winter and autumnal moth larvae (Edland 1971; Tammaru *et al.* 1995) as well as the closely related Bruce spanworm, *Operophtera bruceata* (Brown 1962) show that ballooning rates drop quickly with distance beyond a few hundred metres.

(b) Host plant phenology as a putative Moran effect

So far the most direct evidence for a Moran effect on the spatio-temporal dynamics of forest insects has been derived from the analyses of spatial meteorological data (e.g. temperature), which has shown that synchrony in climatic variables can exhibit similar spatial profiles (i.e. auto-covariance functions) to population synchrony in some species of forest insects (Peltonen *et al.* 2002). In northern Fennoscandia, metrological stations are too few and too poorly interspersed over climate gradients within the outbreak range of birch forest moth to allow a similar comparison. Instead, we used MODIS-NDVI data in order to determine the onset of plant growth in the spring, which provided a full spatial coverage of the focal region. Onset of plant growth also represents a more biologically explicit variable for spring feeding insects than some arbitrarily selected climatic variable. That the temporal match between larvae hatching and budburst is an important determinant for the survival and growth of larvae has long been recognized (Stenseth & Myrsetrud 2002; Van Asch & Visser 2007). Larvae that hatch too early compared with budburst will suffer starvation and increased mortality (Wint 1983; Tikkanen & Julkunen-Tiitto 2003), while late-hatching larvae will experience food of lower quality and suffer reduced growth and fecundity (Van Dongen *et al.* 1997; Haukioja *et al.* 2002). We found that the onset of plant growth in spring has a phase-dependent pattern of spatial synchrony that was similar to that present in the prevalence of defoliation. This suggests that the timing of spring phenology plays a decisive role in the synchrony moth outbreaks on a regional scale in northern Fennoscandia, probably by initiating local population outbreaks simultaneously over a large spatial scale.

The spatio-temporal pattern of birch phenology in northern Fennoscandia is primarily determined by strong geographical (north–south, oceanic–continental) and altitudinal gradients. However, locally within these phenological gradients, onset of the growing season may vary as much as three to five weeks between years with larger variation in oceanic than continental regions (Karlsen *et al.* 2007). In addition, geographical gradients appear to exist in the effect of temperature on the advance of spring phenology. In the continental part of Fennoscandia, a 1°C increase in temperature has been found to correspond to 3–8 days earlier onset of the growing

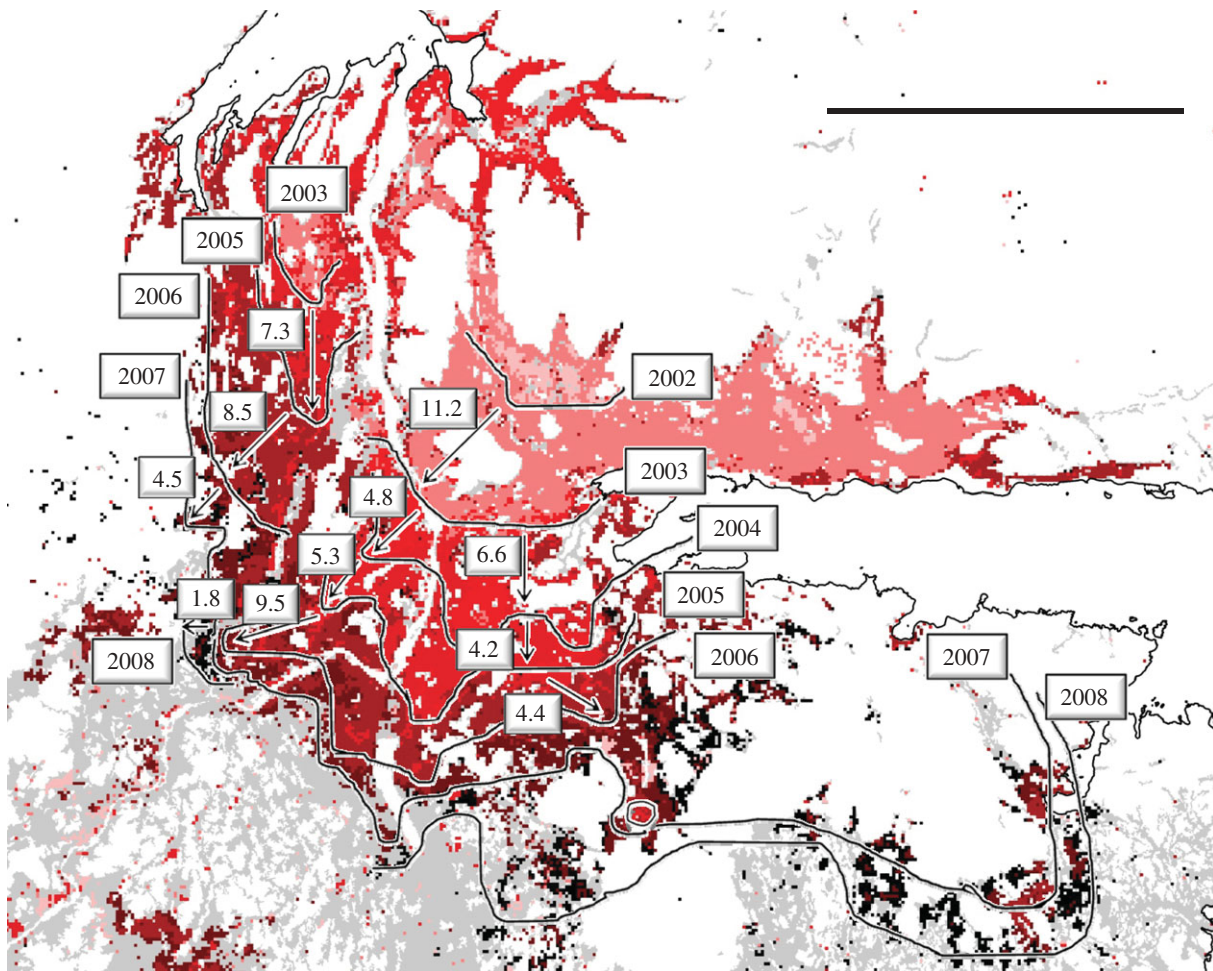


Figure 6. Observed pattern of annual spread of defoliation in the Varanger region ($70^{\circ}15' \text{ N}$, $29^{\circ}0' \text{ E}$) in northeast Norway for the years 2002 (lightest red) to 2008 (darkest red). Black lines show the approximate 'front' of the spread in a southeasterly direction. Numbers in boxes indicate the year and examples of between-year spread distances (in kilometres). Scale bar, 30 km.

season (Karlsson *et al.* 2003; Shutova *et al.* 2006; Pudas *et al.* 2008), while the same temperature increase translates to a 7–10 days earlier onset of the growing season in oceanic northwest Norway (Karlsen *et al.* 2007, 2008). Assuming that larval hatching depends more directly on temperature than does budburst (Topp & Kirsten 1991; Van Asch & Visser 2007), there is a large potential for local and regional differences in the degree of match between larval hatching and birch budburst in individual years. Thus for the observed massive large-scale outbreak to develop, meteorological conditions providing a good phenological match must have occurred simultaneously at a large scale. While we accordingly found evidence for large-scale synchronization of spring phenology during the incipient phase of the cycle, still more research is needed. In particular, aspects of the spring phenology of the moths (egg-hatching time distributions under various temperature regimes) need to be established as to elucidate the exact conditions that provide the necessary phenological matching for outbreaks to take place.

5. CONCLUSION

We have made progress on three aspects of the issue of spatial dynamics of cyclically outbreaking herbivores. First, we have demonstrated a striking phase-dependence in the synchronization of outbreaks of northern birch

forest moths, with evidence for most extensive synchronization and spread taking place in the incipient phase of the outbreak cycle. Second, by modelling outbreak spread distance distributions, we gained more detailed information about the scale of the underlying processes than by only focusing on outbreak synchrony. In particular, we found that the relative importance of long-distance and short-distance spread events shifted among the different phase of the cycles. Third, by analysing satellite-derived data on both forest defoliation and spring phenology, we show that they have matching synchrony-distance profiles. This provides support for the hypothesis that a climate event in the spring influential to phenology of moths and their host plant is likely to act as a Moran effect.

This work was funded by the Department of Biology, University of Tromsø and the Research Council of Norway.

REFERENCES

- Aukema, B. H., Carroll, A. L., Zhu, J., Raffa, K. F., Sickley, T. A. & Taylor, S. W. 2006 Landscape level analysis of mountain pine beetle in British Columbia, Canada: spatiotemporal development and spatial synchrony within the present outbreak. *Ecography* **29**, 427–441. (doi:10.1111/j.2006.0906-7590.04445.x)
- Bates, D. M. & Watts, D. G. 1988 *Nonlinear regression analysis and its applications*. New York, NY: Wiley.

- Beck, P. S. A., Jonsson, P., Hogda, K. A., Karlsen, S. R., Eklundh, L. & Skidmore, A. K. 2007 A ground-validated NDVI dataset for monitoring vegetation dynamics and mapping phenology in Fennoscandia and the Kola peninsula. *Int. J. Remote Sens.* **28**, 4311–4330. (doi:10.1080/01431160701241936)
- Bell, J. R., Bohan, D. A., Shaw, E. M. & Weyman, G. S. 2005 Ballooning dispersal using silk: world fauna, phylogenies, genetics and models. *Bull. Entomol. Res.* **95**, 69–114.
- Berryman, A. A. 1996 What causes population cycles of forest Lepidoptera? *Trends Ecol. Evol.* **11**, 28–32. (doi:10.1016/0169-5347(96)81066-4)
- Bjørnstad, O. N. & Falck, W. 2001 Nonparametric spatial covariance functions: estimation and testing. *Environ. Ecol. Stat.* **8**, 53–70.
- Bjørnstad, O. N., Ims, R. A. & Lambin, X. 1999 Spatial population dynamics: analyzing patterns and processes of population synchrony. *Trends Ecol. Evol.* **14**, 427–432. (doi:10.1016/S0169-5347(99)01677-8)
- Brown, C. E. 1962 The life history and dispersal of the Bruce spanworm, *Operophtera bruceata* (Lep.: Geometridae). *Can. Entomol.* **94**, 1103–1107.
- Bylund, H. 1999 Climate and the population dynamics of two insect outbreak species in the North. *Ecol. Bull.* **47**, 54–62.
- Chesson, P. & Lee, C. T. 2005 Families of discrete kernels for modeling dispersal. *Theoret. Popul. Biol.* **67**, 241–256. (doi:10.1016/j.tpb.2004.12.002)
- Edland, T. 1971 Wind dispersal of the winter moth, *Operophtera brumata* (L.) (Lep. Geometridae) and its relevance to control measures. *Norsk Entomol. Tidsskrift* **18**, 103–105.
- Gilbert, M., Gregoire, J. C., Freise, J. F. & Heitland, W. 2004 Long-distance dispersal and human population density allow the prediction of invasive patterns in the horse chestnut leafminer *Cameraria ohridella*. *J. Anim. Ecol.* **73**, 459–468. (doi:10.1111/j.0021-8790.2004.00820.x)
- Hagen, S. B., Jepsen, J. U., Yoccoz, N. G. & Ims, R. A. 2008 Anisotropic patterned population synchrony in climatic gradients indicates nonlinear climatic forcing. *Proc. R. Soc. B* **275**, 1509–1515. (doi:10.1098/rsph.2008.0122)
- Hämet-Ahti, L. 1963 Zonation of the mountain birch forests in northernmost Fennoscandia. *Ann. Bot. Soc. Zool. Bot. Fennica* **34**, 1–127.
- Haukioja, E., Neuvonen, S., Hanhimäki, S. & Niemelä, P. 1988 The autumnal moth in Fennoscandia. In *Dynamics of forest insect populations: patterns, causes and management strategies* (ed. A. A. Berryman), pp. 163–177. New York, NY: Academic Press.
- Haukioja, E., Ossipov, V. & Lempa, K. 2002 Interactive effects of leaf maturation and phenolics on consumption and growth of a geometrid moth. *Entomol. Experimental Appl.* **104**, 125–136. (doi:10.1023/A:1021280106023)
- Haydon, D. T., Greenwood, P. E., Stenseth, N. C. & Saitoh, T. 2003 Spatio-temporal dynamics of the grey-sided vole in Hokkaido: identifying coupling using state-based Markov-chain modelling. *Proc. R. Soc. Lond. B* **270**, 435–445. (doi:10.1098/rsph.2002.2230)
- Huete, A., Didan, K., Miura, T., Rodriguez, E. P., Gao, X. & Ferreira, L. G. 2002 Overview of the radiometric and biophysical performance of the MODIS vegetation indices. *Remote Sens. Environ.* **83**, 195–213. (doi:10.1016/S0034-4257(02)00096-2)
- Ims, R. A., Yoccoz, N. G. & Hagen, S. B. 2004 Do sub-Arctic winter moth populations in coastal birch forest exhibit spatially synchronous dynamics? *J. Anim. Ecol.* **73**, 1129–1136. (doi:10.1111/j.0021-8790.2004.00882.x)
- Jepsen, J. U., Hagen, S. B., Høgda, K. A., Ims, R. A., Karlsen, S. R., Tømmervik, H. & Yoccoz, N. G. 2009 Monitoring the spatio-temporal dynamics of geometrid moth outbreaks in birch forest using MODIS-NDVI data. *Remote Sens. Environ.* **13**, 1939–1947.
- Johansen, B. & Karlsen, S. R. 2005 Monitoring vegetation changes on Finnmarksvidda, Northern Norway, using Landsat MSS and Landsat TM/ETM+ satellite images. *Phytocoenologia* **35**, 969–984. (doi:10.1127/0340-269X/2005/0035-0969)
- Johnson, D. M., Liebhold, A. M., Tobin, P. C. & Bjørnstad, O. N. 2006 Allele effects and pulsed invasion by the gypsy moth. *Nature* **444**, 361–363. (doi:10.1038/nature05242)
- Kallio, P. & Lehtonen, J. 1973 Birch forest damage caused by *Oporina autumnata* (Bkh.) in 1966–99 in Utsjoki. Reports from Kevo Subarctic Research Station, vol. 10, pp. 55–69.
- Karlsen, S. R., Elvebakk, A., Hogda, K. A. & Johansen, B. 2006 Satellite-based mapping of the growing season and bioclimatic zones in Fennoscandia. *Global Ecol. Biogeogr.* **15**, 416–430. (doi:10.1111/j.1466-822X.2006.00234.x)
- Karlsen, S. R., Solheim, I., Beck, P. S. A., Hogda, K. A., Wielgolaski, F. E. & Tømmervik, H. 2007 Variability of the start of the growing season in Fennoscandia, 1982–2002. *Int. J. Biometeorol.* **51**, 513–524. (doi:10.1007/s00484-007-0091-x)
- Karlsen, S. R. *et al.* 2008 MODIS-NDVI-based mapping of the length of the growing season in northern Fennoscandia. *Int. J. Appl. Earth Obs. Geoinform.* **10**, 253–266. (doi:10.1016/j.jag.2007.10.005)
- Karlsen, S. R., Ramfjord, H., Hogda, K. A., Johansen, B., Danks, F. S. & Brobakk, T. E. 2009 A satellite-based map of onset of birch (*Betula*) flowering in Norway. *Aerobiologia* **25**, 15–25. (doi:10.1007/s10453-008-9105-3)
- Karlsso, P. S., Bylund, H., Neuvonen, S., Heino, S. & Tjus, M. 2003 Climatic response of budburst in the mountain birch at two areas in northern Fennoscandia and possible responses to global change. *Ecography* **26**, 617–625. (doi:10.1034/j.1600-0587.2003.03607.x)
- Klemola, T., Huitu, O. & Ruohomäki, K. 2006 Geographically partitioned spatial synchrony among cyclic moth populations. *Oikos* **114**, 349–359. (doi:10.1111/j.2006.0030-1299.14850.x)
- Klemola, T., Andersson, T. & Ruohomäki, K. 2008 Fecundity of the autumnal moth depends on pooled geometrid abundance without a time lag: implications for cyclic population dynamics. *J. Anim. Ecol.* **77**, 597–604. (doi:10.1111/j.1365-2656.2008.01369.x)
- Kot, M., Lewis, M. A. & Van den Driessche, P. 1996 Dispersal data and the spread of invading organisms. *Ecology* **77**, 2027–2042. (doi:10.2307/2265698)
- Lehtonen, J. & Heikkinen, R. K. 1995 On the recovery of mountain birch after *Epirrita* damage in Finnish Lapland, with a particular emphasis on reindeer grazing. *Ecoscience* **2**, 349–356.
- Liebhold, A. & Kamata, N. 2000 Introduction: are population cycles and spatial synchrony a universal characteristic of forest insect populations? *Popul. Ecol.* **42**, 205–209. (doi:10.1007/PL00011999)
- Liebhold, A. M. & Tobin, P. C. 2008 Population ecology of insect invasions and their management. *Ann. Rev. Entomol.* **53**, 387–408. (doi:10.1146/annurev.ento.52.110405.091401)
- Liebhold, A. M., Halverson, J. A. & Elmes, G. A. 1992 Gypsy moth invasion in North America: a quantitative analysis. *J. Biogeogr.* **19**, 513–520. (doi:10.2307/2845770)
- Liebhold, A., Koenig, W. D. & Bjørnstad, O. N. 2004 Spatial synchrony in population dynamics. *Ann. Rev. Ecol. Syst.* **35**, 467–490. (doi:10.1146/annurev.ecolsys.34.011802.132516)

- Myers, J. H. 1988 Can a general hypothesis explain population-cycles of forest Lepidoptera? *Adv. Ecol. Res.* **18**, 179–242. (doi:10.1016/S0065-2504(08)60181-6)
- Nilssen, A. C., Tenow, O. & Bylund, H. 2007 Waves and synchrony in *Epirrita autumnata/Operophtera brumata* outbreaks. II. Sunspot activity cannot explain cyclic outbreaks. *J. Anim. Ecol.* **76**, 269–275. (doi:10.1111/j.1365-2656.2006.01205.x)
- Peltonen, M., Liebhold, A. M., Bjørnstad, O. N. & Williams, D. W. 2002 Spatial synchrony in forest insect outbreaks: roles of regional stochasticity and dispersal. *Ecology* **83**, 3120–3129.
- Pudas, E., Tolvanen, A., Poikolainen, J., Sukuvaara, T. & Kubin, E. 2008 Timing of plant phenophases in Finnish Lapland in 1997–2006. *Boreal Environ. Res.* **13**, 31–43.
- Ruohomäki, K., Tanhuanpää, M., Ayres, M. P., Kaitaniemi, P., Tammaru, T. & Haukioja, E. 2000 Causes of cyclicity of *Epirrita autumnata* (Lepidoptera, Geometridae): grandiose theory and tedious practice. *Popul. Ecol.* **42**, 211–223. (doi:10.1007/PL00012000)
- Sharov, A. A. & Liebhold, A. M. 1998 Model of slowing the spread of gypsy moth (Lepidoptera: Lymantriidae) with a barrier zone. *Ecol. Appl.* **8**, 1170–1179. (doi:10.1890/1051-0761(1998)008[1170:MOSTSO]2.0.CO;2)
- Sherratt, J. A. & Smith, M. J. 2008 Periodic travelling waves in cyclic populations: field studies and reaction-diffusion models. *J. R. Soc. Interface* **5**, 483–505. (doi:10.1098/rsif.2007.1327)
- Shutova, E. *et al.* 2006 Growing seasons of Nordic mountain birch in northernmost Europe as indicated by long-term field studies and analyses of satellite images. *Int. J. Biometeorol.* **51**, 155–166. (doi:10.1007/s00484-006-0042-y)
- Stenseth, N. C. & Mysterud, A. 2002 Climate, changing phenology, and other life history and traits: nonlinearity and match-mismatch to the environment. *Proc. Natl Acad. Sci. USA* **99**, 13379–13381. (doi:10.1073/pnas.121519399)
- Tammaru, T., Kaitaniemi, P. & Ruohomäki, K. 1995 Oviposition choices of *Epirrita autumnata* (Lepidoptera: Geometridae) in relation to its eruptive population dynamics. *Oikos* **74**, 296–304. (doi:10.2307/3545659)
- Tanhuanpää, M., Ruohomäki, K., Turchin, P., Ayres, M. P., Bylund, H., Kaitaniemi, P., Tammaru, T. & Haukioja, E. 2002 Population cycles of the autumnal moth in Fennoscandia. In *Population cycles: the case for trophic interactions* (ed. A. A. Berryman), pp. 142–154. Oxford, UK: Oxford University Press.
- Tenow, O. 1972 The outbreaks of *Oporinia autumnata* Bkh. and *Operophtera* spp. (Lep., Geometridae) in the Scandinavian mountain chain and Northern Finland 1862–1968. *Zool. Bidrag från Uppsala* (Suppl. 2), 1–107.
- Tenow, O. & Bylund, H. 2000 Recovery of a *Betula pubescens* forest in northern Sweden after severe defoliation by *Epirrita autumnata*. *J. Veg. Sci.* **11**, 855–862. (doi:10.2307/3236555)
- Tenow, O., Nilssen, A. C., Bylund, H. & Hogstad, O. 2007 Waves and synchrony in *Epirrita autumnata/Operophtera brumata* outbreaks. I. Lagged synchrony: regionally, locally and among species. *J. Anim. Ecol.* **76**, 258–268. (doi:10.1111/j.1365-2656.2006.01204.x)
- Tikkanen, O. P. & Julkunen-Tiitto, R. 2003 Phenological variation as protection against defoliating insects: the case of *Quercus robur* and *Operophtera brumata*. *Oecologia* **136**, 244–251. (doi:10.1007/s00442-003-1267-7)
- Tobin, P. C., Liebhold, A. M. & Roberts, E. A. 2007 Comparison of methods for estimating the spread of a non-indigenous species. *J. Biogeogr.* **34**, 305–312. (doi:10.1111/j.1365-2699.2006.01600.x)
- Topp, W. & Kirsten, K. 1991 Synchronization of preimaginal development and reproductive success in the winter moth, *Operophtera brumata* L. *J. Appl. Entomol.-Zeitschrift Für Angewandte Entomologie* **111**, 137–146.
- Van Asch, M. & Visser, M. E. 2007 Phenology of forest caterpillars and their host trees: the importance of synchrony. *Ann. Rev. Entomol.* **52**, 37–55. (doi:10.1146/annurev.ento.52.110405.091418)
- Van Dongen, S., Backeljau, T., Matthysen, E. & Dhondt, A. A. 1997 Synchronization of hatching date with budburst of individual host trees (*Quercus robur*) in the winter moth (*Operophtera brumata*) and its fitness consequences. *J. Anim. Ecol.* **66**, 113–121.
- Väre, H. 2001 Mountain birch taxonomy and floristics of mountain birch woodlands. In *Mountain birch forest ecosystems*, vol. 27 (ed. F. E. Wielgolaski), pp. 35–46. Paris, France: UNESCO.
- Wiens, J. A. 1989 Spatial scaling in ecology. *Func. Ecol.* **3**, 385–397. (doi:10.2307/2389612)
- Wint, W. 1983 The role of alternative host-plant species in the life of a polyphagous moth, *Operophtera brumata* (Lepidoptera, Geometridae). *J. Anim. Ecol.* **52**, 439–450.